# The conoRFamide RPRFa stabilizes the open conformation of Acid-Sensing Ion Channel 3 via the nonproton ligand sensing domain

Melissa Reiners, Michael A. Margreiter, Adrienne Oslender-Bujotzek, Giulia Rossetti, Stefan Gründer, and Axel Schmidt

Molecular Pharmacology

**Supporting Information**

**Supplemental Figure 1. Knowledge-based homology model of rat ASIC3 in the open conformation.**

**Supplemental Figure 2. Knowledge-based homology model of rat ASIC3 in the desensitized conformation.**

**Supplemental Figure 3. Knowledge-based homology model of rat ASIC3 in the open conformation in complex with RPRFa in its best-ranked docking pose.**

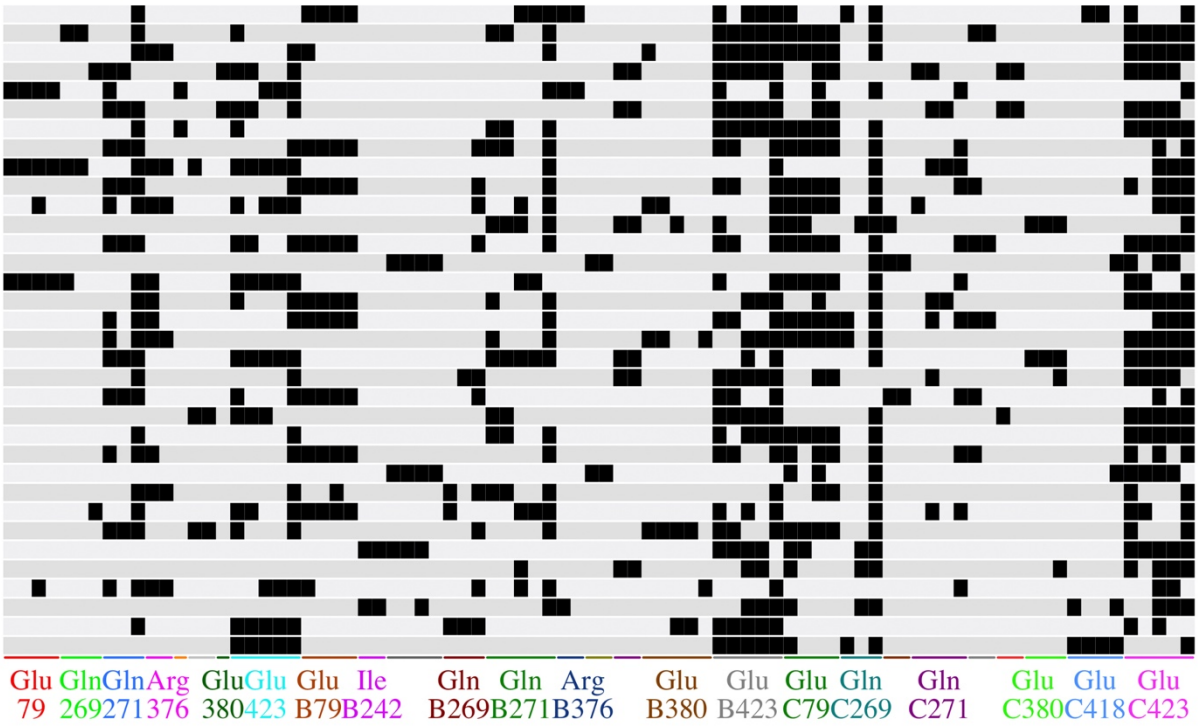


**Supplemental Figure 4. Protein-ligand interaction fingerprint (PLIF) shown in Fig. 4 in barcode representation.** All receptor amino acids that form at least one protein-peptide interaction are listed. A row represents one particular binding pose and interactions are highlighted as black squares. Better scoring poses are on the top (more negative Emodel scores). Depending on the interacting receptor amino acid, several different interactions (e.g. salt bridges, π-stacking) can be formed. Thus, there are varying numbers of corresponding columns.

**Supplemental Figure 5. Movie showing from different perspectives the homology model of ASIC3 in the open conformation in complex with RPRFa in its best-ranked docking pose.**

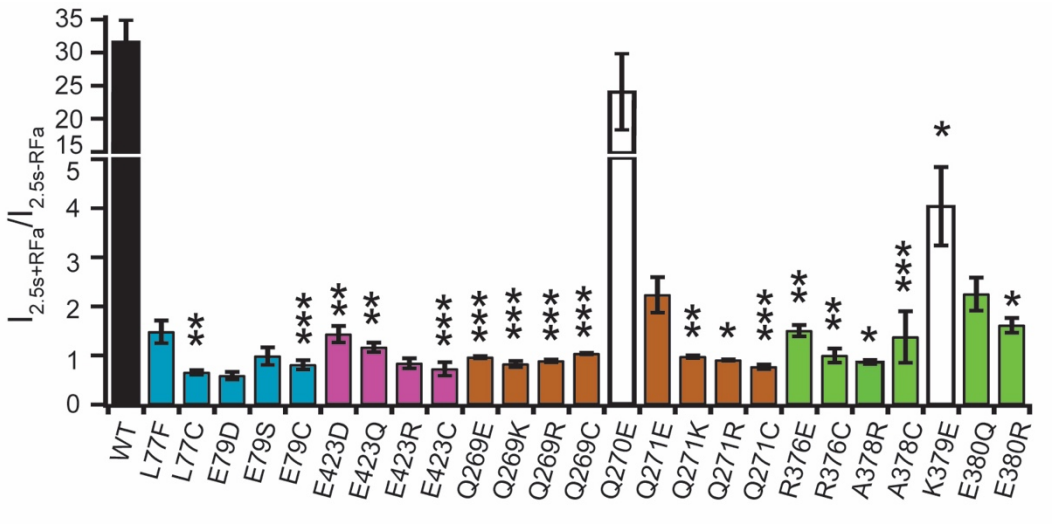


**Supplemental Figure 6. Mean $I_{2.5s+RFa}/I_{2.5s}$ ratios for all 25 mutants of the NPLSD.** Bar graph showing mean ratios of current amplitudes 2.5 sec post-peak in the absence of and after pre-incubation with RPRFamide ($I_{2.5s+RFa}/I_{2.5s}$). Bars are shown in the colour of the corresponding β strands in Fig. 5A; the white bars represent residues whose side chains point away from the cavity. Note that the y-axis has two different scales. Error bars indicate SEM. $n_{mutant}$ = 8-19; $n_{wt}$ = 4-28 (each condition), $n_{wt}$ (total) = 102. *, $P < 0.05$; **, $P < 0.01$; ***, $P < 0.001$ (Student´s t-test followed by Bonferroni correction).

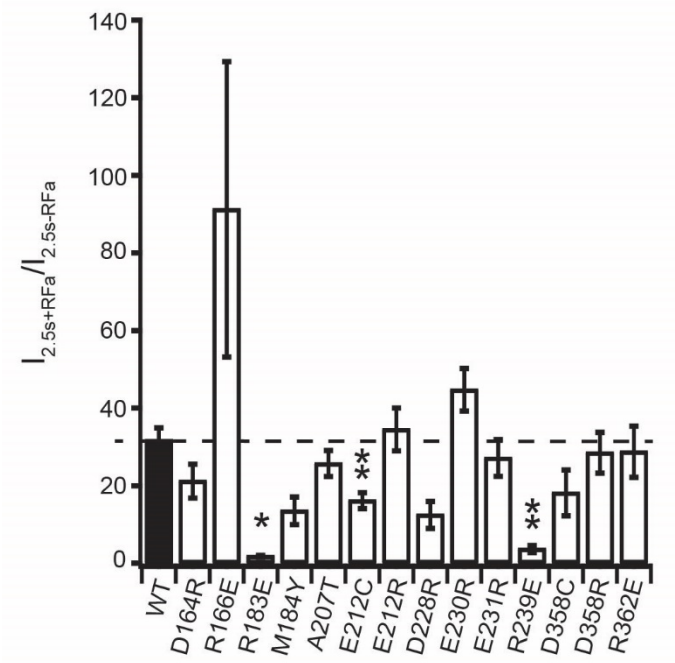


**Supplemental Figure 7. Mean $I_{2.5s+RFa}/I_{2.5s}$ ratios for all 12 mutants of the acidic pocket.** The dotted line represents the ratio of the wild type as reference. Error bars indicate SEM. $n_{mutant}$ = 8-18; $n_{wt}$ = 6-20 (each condition), $n_{wt}$ (total) = 102. *, $P < 0.05$; **, $P < 0.01$ (Student´s t-test followed by Bonferroni correction).

| SiteMap Results | | SiteScore | Volume (Å$^3$) |
|---|---|---|---|
| **Open Model** | Site #1 (AP) | 1.10 | 820 |
| | Site #2 (NPLSD) | 1.06 | 3484 |
| | Site #3 | 1.03 | 884 |
| | Site #4 | 1.02 | 919 |
| | Site #5 | 1.00 | 968 |
| **Desensitized Model** | Site #1 (AP1) | 1.11 | 631 |
| | Site #2 | 1.10 | 497 |
| | Site #3 (AP2) | 1.08 | 700 |
| | Site #4 | 1.00 | 874 |
| | Site #5 | 0.99 | 1180 |

**Supplemental Table 1. Potential binding sites on ASIC3.** Binding sites were detected with SiteMap (see Methods). SiteScore values and volume of the sites are indicated. Potential binding sites were sorted according to SiteScore for the individual models. The NPLSD is only detected in the open state model. The acidic pocket (AP) is detected twice in the desensitized state model, due to receptor symmetry. In the open state model, the AP is ranked slightly higher than the NPLSD.

| RPRFamide Conformer | Docking Score | Glide Emodel Score |
|---|---|---|
| **1** | -7.28 | -110.92 |
| **2** | -8.26 | -109.83 |
| **3** | -8.30 | -105.80 |
| **4** | -5.02 | -102.57 |
| **5** | -6.33 | -101.56 |
| **6** | -5.75 | -93.37 |
| **7** | -6.80 | -91.31 |
| **8** | -5.53 | -91.15 |
| **9** | -5.37 | -90.17 |
| **10** | -5.51 | -88.82 |
| **11** | -6.80 | -88.74 |
| **12** | -5.75 | -88.62 |
| **13** | -5.76 | -88.53 |
| **14** | -4.51 | -83.92 |
| **15** | -5.52 | -83.06 |
| **16** | -5.76 | -82.05 |
| **17** | -5.41 | -81.59 |
| **18** | -5.59 | -77.51 |
| **19** | -6.23 | -76.98 |
| **20** | -6.57 | -76.21 |
| **21** | -4.62 | -75.22 |
| **22** | -4.78 | -73.97 |
| **23** | -6.54 | -73.51 |
| **24** | -4.50 | -66.57 |
| **25** | -3.20 | -66.21 |
| **26** | -4.31 | -64.91 |
| **27** | -5.28 | -64.48 |
| **28** | -5.33 | -64.16 |
| **29** | -5.58 | -63.72 |
| **30** | -3.13 | -61.05 |
| **31** | -4.87 | -57.34 |
| **32** | -4.28 | -57.13 |
| **33** | -4.28 | -54.60 |
| **34** | -6.49 | -54.27 |

**Supplemental Table 2. Docking scores of RPRFamide binding poses.**

| Mutant | $I_{pH6.3}$ (μA) | $[I_{2.5s+RFa} - I_{2.5s-RFa}]/I_{pH6.3}$ | $I_{2.5s+RFa}/I_{2.5s-RFa}$ | $I_{pH6.3} / I_{pH4.0}$ | n |
|---|---|---|---|---|---|
| **WT** | -11.0±1.0 | 0.28±0.03 | 31.68±3.27 | 0.55±0.02 | 100-102 |
| **L77C** | -5.3±1.2** | -0.06±0.01*** | 0.66±0.04** | 0.30±0.02*** | 11 |
| **L77F** | -6.3±1.3 | 0±0* | 1.50±0.21 | 0.27±0.03** | 11 |
| **E79D** | -0.1±0* | -0.60±0.18*** | 0.59±0.08 | 0.15±0.02*** | 10 |
| **E79S** | -0.5±0.2 | -0.01±0.05 | 1.03±0.16 | 0.12±0.02*** | 11 |
| **E79C** | -0.6±0.1*** | -0.06±0.04*** | 0.81±0.09*** | 0.23±0.02*** | 17 |
| **E423D** | -0.3±0.1** | 0.05±0.02** | 1.43±0.16** | 0.22±0.02*** | 19 |
| **E423Q** | -7.7±2.4 | 0±0 | 1.17±0.10** | 0.31±0.06 | 10 |
| **E423R** | -0.2±0* | -0.05±0.03*** | 0.81±0.10 | 0.10±0.02*** | 12 |
| **E423C** | -1.1±0.4*** | -0.15±0.06** | 0.73±0.14*** | 0.22±0.07** | 8 |
| **Q269C** | -8.4±1.9** | 0.03±0.01*** | 1.04±0.02*** | 0.54±0.03* | 14 |
| **Q269E** | -0.9±0.2*** | -0.04±0.02*** | 0.96±0.03*** | 0.78±0.04 | 12 |
| **Q269K** | -19.1±2.8 | -0.13±0.05*** | 0.82±0.06*** | 0.52±0.03 | 11 |
| **Q269R** | -13.8±2.6 | -0.02±0*** | 0.89±0.03*** | 0.49±0.06 | 12 |
| **Q270E** | -1.8±0.4*** | 0.23±0.03 | 24.15±5.74 | 0.30±0.03*** | 11 |
| **Q271E** | -3.7±1.0 | 0.06±0.02 | 2.24±0.36 | 0.49±0.07 | 10 |
| **Q271K** | -17.6±2.3 | -0.02±0.02*** | 0.97±0.03** | 0.82±0.03 | 11 |
| **Q271R** | -16.8±2.8*** | -0.08±0.01*** | 0.91±0.01* | 0.65±0.05** | 17-18 |
| **Q271C** | -1.4±0.3*** | -0.23±0.05*** | 0.77±0.05*** | 0.44±0.01*** | 17-18 |
| **R376E** | -3.5±0.5 | 0.04±0.01*** | 1.50±0.12** | 0.58±0.04* | 9 |
| **R376C** | -0.2±0** | -0.1±0.04*** | 1.00±0.14** | 0.45±0.05 | 14-16 |
| **A378R** | -8.2±2.1 | -0.01±0*** | 0.87±0.04* | 0.47±0.03 | 14 |
| **A378C** | -0.8±0.4*** | 0.02±0.06 | 1.38±0.53*** | 0.32±0.04** | 11 |
| **K379E** | -0.2±0** | 0.26±0.05 | 4.04±0.80* | 0.15±0.03** | 9 |
| **E380Q** | -15.9±2.5* | 0.06±0.02 | 2.25±0.34 | 0.39±0.04 | 11 |
| **E380R** | -0.3±0.1** | 0.17±0.03** | 1.61±0.15* | 0.08±0.01*** | 9 |
| | | | | | |
| **D164R** | -10.5±1.8 | 0.2±0.03 | 21.14±4.41 | 0.51±0.04 | 9 |
| **R166E** | -2.5±0.8** | 0.25±0.03 | 91.22±38.07 | 0.59±0.05 | 11-12 |
| **R183E** | -0.6±0.4 | 0.21±0.05 | 1.83±0.21* | 0.05±0.02*** | 8 |
| **M184Y** | -1.3±0.6 | 0.2±0.02 | 13.56±3.59 | 0.30±0.02*** | 12 |
| **A207T** | -24.2±5.3 | 0.31±0.05 | 25.69±3.37 | 0.79±0.06 | 10 |
| **E212R** | -6.9±2.4 | 0.46±0.04 | 34.49±5.54 | 0.17±0.04*** | 9 |
| **E212C** | -0.6±0.2 | 0.61±0.04 | 16.11±2.07** | 0.10±0.01** | 9 |
| **D228R** | -2.6±0.9 | 0.37±0.07 | 12.45±3.49 | 0.50±0.04 | 8 |
| **E230R** | -3.7±1.3 | 0.37±0.05 | 44.70±5.47 | 0.44±0.06 | 9 |
| **E231R** | -3.2±0.7** | 0.49±0.10 | 27.15±4.72 | 0.19±0.01*** | 18 |
| **R239E** | -1.5±0.6** | 0.27±0.07 | 3.70±0.95** | 0.22±0.08 | 10 |
| **D358R** | -5.6±1.4 | 0.31±0.04 | 28.49±5.27 | 0.53±0.05 | 11 |
| **D358C** | -3.9±1.0 | 0.27±0.03 | 18.12±5.89 | 0.57±0.04 | 9 |
| **R362E** | -4.9±3.0 | 0.45±0.05 | 28.76±6.63 | 0.22±0.05* | 12 |

**Supplemental Table 3. Data obtained in the experiments shown in figures 5 and 7.** Values are reported as mean ± S.E.M. *, $P < 0.05$; **, $P < 0.01$; ***, $P < 0.001$ (unpaired t-test between recordings of mutants and wild type of the same week followed by Bonferroni correction).

| Mutant | $I_{pH\ 6.3}$ (µA) | $[I_{0.5s+RFa} - I_{0.5s-RFa}]/I_{pH6.3}$ | $I_{0.5s+RPRFa}/I_{0.5s-RPRFa}$ | $a_2$ | $\tau_1$ | $\tau_2/\tau_1$ | n |
|---|---|---|---|---|---|---|---|
| **WT** | -13.6±2.0 | 0.90±0.07 | 4.96±0.50 | 0.91±0.03 | 0.30±0.01 | 22.0±1.4 | 15-17 |
| **L77F** | -5.6±1.6 | 0.33±0.05*** | 2.96±0.24 | 0.69±0.07 | 0.29±0.06 | 4.6±0.4*** | 10 |
| **L77C** | -1.6±0.6* | 0.17±0.04*** | 1.41±0.08** | 0.19±0.01*** | 0.43±0.06 | 9.6±0.9*** | 6 |
| **E79S** | -1.7±0.3** | 0.29±0.04*** | 7.25±8.26 | 0.67±0.05** | 0.08±0*** | 3.9±0.2*** | 8 |
| **E423D** | -0.2±0.1*** | 1.11±0.25 | 4.93±0.56 | 0.76±0.07 | 0.60±0.19 | 9.9±1.9*** | 9 |
| **E423R** | -0.2±0*** | -0.01±0.02*** | 0.98±0.21*** | 0.57±0.21 | 0.10±0.01*** | 8.9±6.6 | 9 |
| **Q269R** | -16.2±5.0 | 0.22±0.02*** | 1.64±0.05*** | 0.73±0.06 | 0.31±0.02 | 11.1±0.7*** | 9 |
| **Q269C** | -4.2±1.0 | 0.51±0.07* | 1.70±0.13** | 0.82±0.05 | 0.95±0.36 | 8.4±2.1*** | 7-8 |
| **Q271R** | -17.7±3.5 | -0.10±0.01*** | 0.89±0.02*** | | | | 12 |
| **R376E** | -5.4±1.5 | 0.17±0.04*** | 1.35±0.09*** | 0.17±0.02*** | 0.53±0.04*** | 10.1±0.7*** | 7-8 |
| **A378R** | -9.0±2.8 | 0.04±0.02*** | 1.25±0.07*** | 0.46±0.16* | 0.20±0.02** | 2.2±0.4*** | 7-12 |
| **A378C** | -4.4±1.9 | 0.17±0.05*** | 1.45±0.08** | 0.44±0.08*** | 0.53±0.22 | 9.3±2.7** | 8 |
| **E380Q** | -2.4±0.7** | 0.49±0.05** | 3.98±0.26 | 0.88±0.04 | 0.24±0.02 | 9.3±0.5*** | 9 |

**Supplemental Table 4. Data obtained in the experiments shown in figure 6.** Values are reported as mean ± S.E.M. *, $P < 0.05$; **, $P < 0.01$; ***, $P < 0.001$ (unpaired t-test followed by Bonferroni correction). Mutant Q271R could not be fitted by a bi-exponential fit.